

# Thermally assisted spin transfer torque switching in synthetic free layers

Tomohiro Taniguchi<sup>1,2</sup> and Hiroshi Imamura<sup>1</sup>

<sup>1</sup> *Nanosystem Research Institute, National Institute of Advanced Industrial Science and Technology, Tsukuba, Ibaraki 305-8568, Japan,*

<sup>2</sup> *Institute of Applied Physics, University of Tsukuba, Tsukuba, Ibaraki 305-8573, Japan*

(Dated: November 11, 2018)

We studied the magnetization reversal rates of thermally assisted spin transfer torque switching in a synthetic free layer theoretically. By solving the Fokker-Planck equation, we obtained the analytical expression of the switching probability for both the weak and the strong coupling limit. We found that the thermal stability is proportional to  $\Delta_0(1 - I/I_c)^2$ , not  $\Delta_0(1 - I/I_c)$  as argued by Koch *et al.* [Phys. Rev. Lett. **92**, 088302 (2004)], where  $I$  and  $I_c$  are the electric current and the critical current of spin transfer torque switching at absolute zero temperature, respectively. The difference in the exponent of  $(1 - I/I_c)$  leads to a significant underestimation of the thermal stability  $\Delta_0$ . We also found that fast switching is achieved by choosing the appropriate direction of the applied field.

PACS numbers: 75.76.+j, 75.75.-c, 85.75.-d

## I. INTRODUCTION

Spin transfer torque switching of the magnetization in ferromagnetic nanostructures has been extensively studied both theoretically<sup>1-3</sup> and experimentally<sup>4-7</sup> because of its potential application to spin-electronics devices such as magnetic random access memory. For device applications, a thermal stability  $\Delta_0 = MH_{\text{an}}V/(2k_B T)$  of more than 40 is required to guarantee retention time of longer than ten years, where  $M$ ,  $H_{\text{an}}$ ,  $V$ ,  $k_B$  and  $T$  are the magnetization, the anisotropy field, the volume of the free layer, the Boltzmann constant, and the temperature, respectively.

Recently, Hayakawa *et al.*<sup>8</sup> showed that the anti-ferromagnetically coupled synthetic free layer, CoFeB(2.6nm)/Ru(0.8nm)/CoFeB(2.6nm), in a CoFeB(fixed layer)/MgO/CoFeB/Ru/CoFeB magnetic tunnel junction shows a large thermal stability ( $\Delta_0 > 80$ ) compared to a single free layer. On the other hand, Yakata *et al.*<sup>9,10</sup> showed that a ferromagnetically coupled CoFeB/Ru/CoFeB synthetic free layer shows a large thermal stability ( $\Delta_0 = 146 \pm 29$  for CoFeB(2nm)/Ru(1.5nm)/CoFeB(2nm) and  $248 \pm 60$  for CoFeB(2nm)/Ru(1.5nm)/CoFeB(4nm)) compared to the single and the anti-ferromagnetically coupled synthetic free layer. These intriguing results spurred us to study a thermally assisted spin transfer torque switching in synthetic free layer. In contrast to the large number of experimental studies<sup>8-10</sup>, few theoretical studies have been reported. Although the analytical expression of the switching rate of the thermally assisted spin transfer torque switching for the single free layer<sup>11-13</sup>,  $P = 1 - \exp[-f_0 t \exp\{-\Delta_0(1 - I/I_c)(1 - H_{\text{appl}}/H_{\text{an}})^2\}]$ , has been widely used to fit the experiments [see Eqs. (1)-(3) in Refs.<sup>9,10</sup>], where  $I_c$  is the critical current of the spin transfer torque switching at absolute zero temperature, it is not clear whether this single layer formula has validity when applied to a synthetic free layer. Thus, it is important to derive an analytical

expression of the switching rate of the thermally assisted spin transfer torque switching for the synthetic free layer.

In this paper, we studied the thermally assisted spin transfer torque switching rate for a synthetic free layer by solving the Fokker-Planck equation. The analytical expressions of the switching rate were obtained for weak and strong coupling limits of the  $F_1$  and  $F_2$  layers. One of the main findings was that the dependence of the thermal stability  $\Delta$  on the current  $I$  is given by  $\Delta \propto \Delta_0(1 - I/I_c)^2$ , not  $(1 - I/I_c)$ , as argued by the previous authors:<sup>11</sup> We emphasize that even for the single free layer  $\Delta$  is proportional to  $(1 - I/I_c)^2$ . The difference in the exponent of the factor  $(1 - I/I_c)$  leads to a significant underestimation of the thermal stability  $\Delta_0$ . We found that in the presence of the applied field  $H_{\text{appl}}$ , the switching times of the anti-ferromagnetically and the ferromagnetically coupled synthetic layers are different, and that fast switching is achieved by choosing an appropriate direction of  $H_{\text{appl}}$ .

This paper is organized as follows. In Sec. II, we introduce the Fokker-Planck equation for the synthetic free layer and its steady state solution. We also introduce approximations to obtain the analytical expression of the switching probability. In Secs. III and IV, we present the calculation of the switching probability in the limits of the weak and the strong coupling of the  $F_1$  and  $F_2$  layers. In Sec. V, we compare our results with those of other works. Section VI summarizes our findings.

## II. FOKKER-PLANCK EQUATION FOR A SYNTHETIC FREE LAYER

Let us first derive the Fokker-Planck equation for the synthetic free layer. The system we consider is schematically shown in Fig. 1. The two ferromagnetic layers,  $F_1$  and  $F_2$ , consist of a synthetic free layer with the coupling energy  $-JS\mathbf{m}_1 \cdot \mathbf{m}_2$ . Here  $\mathbf{m}_k = \mathbf{M}_k/M_k =$

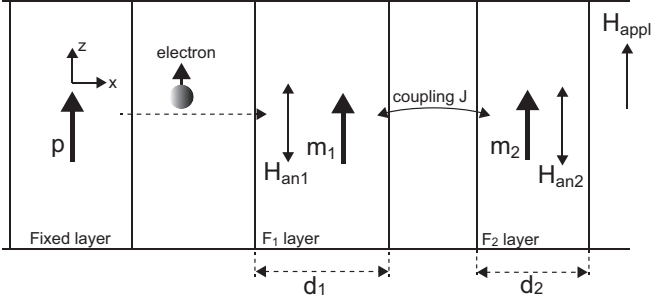


FIG. 1: The schematic view of the synthetic free layer consisting of the  $F_1$  and  $F_2$  layers.  $\mathbf{m}_k$  and  $\mathbf{p}$  are the unit vectors along the directions of the magnetizations in the  $F_k$  and the fixed layers, respectively, and  $d_k$  is the thickness of the  $F_k$  layer.  $H_{\text{appl}}$ ,  $H_{\text{an}}$ , and  $J$  represent the applied field, the anisotropy field, and the coupling between the  $F_1$  and  $F_2$  layers, respectively. The flow of the electrons along the  $+x$  direction corresponds to the negative electric current  $I < 0$ .

$(\sin \theta_k \cos \varphi_k, \sin \theta_k \sin \varphi_k, \cos \theta_k)$  is the unit vector along the direction of the magnetization  $\mathbf{M}_k$  of the  $F_k$  layer.  $J$  and  $S$  are the coupling energy per unit area and the cross-sectional area of the system, respectively. It should be noted that  $J > 0$  and  $J < 0$  correspond to the ferromagnetically coupled and antiferromagnetically coupled synthetic free layers, respectively. Although we consider the ferromagnetically coupled system below, our formalism is applicable to the antiferromagnetically coupled system by changing the sign of the coupling constant  $J$ . We assume the uniaxial anisotropy along the  $z$  axis for both  $F_1$  and  $F_2$  layers, and the magnetizations  $\mathbf{m}_1$  and  $\mathbf{m}_2$  point to the positive  $z$  direction in the initial states. We also assume that the external field  $H_{\text{appl}}$  is applied along the  $z$  axis. Then, the total free energy  $F$  of the  $F_1$  and  $F_2$  layers are given by

$$\begin{aligned}
 F = & -M_1 H_{\text{appl}} V_1 \cos \theta_1 - \frac{1}{2} M_1 H_{\text{an1}} V_1 \cos^2 \theta_1 \\
 & - M_2 H_{\text{appl}} V_2 \cos \theta_2 - \frac{1}{2} M_2 H_{\text{an2}} V_2 \cos^2 \theta_2 \\
 & + 2\pi M_1^2 V_1 (\sin \theta_1 \cos \varphi_1)^2 + 2\pi M_2^2 V_2 (\sin \theta_2 \cos \varphi_2)^2 \\
 & - JS [\sin \theta_1 \sin \theta_2 \cos(\varphi_1 - \varphi_2) + \cos \theta_1 \cos \theta_2], \quad (1)
 \end{aligned}$$

where  $H_{\text{ank}}$ ,  $V_k = Sd_k$  and  $d_k$  are the uni-axial anisotropy field, the volume and the thickness of the  $F_k$  layer, respectively. The fifth and sixth terms in Eq. (1) represent the magnetic energy due to the demagnetization field. We assume that  $|H_{\text{appl}}| < H_{\text{ank}}$  to guarantee at least two local minima of the free energy. When  $H_{Jk} \ll H_{\text{ank}}$ , the states  $(\mathbf{m}_1, \mathbf{m}_2) = (\mathbf{e}_z, \mathbf{e}_z)$ ,  $(\mathbf{e}_z, -\mathbf{e}_z)$ ,  $(-\mathbf{e}_z, \mathbf{e}_z)$ , and  $(-\mathbf{e}_z, -\mathbf{e}_z)$  correspond to the energy minima, where  $H_{Jk} = J/(M_k d_k)$ . On the other hand, when  $H_{Jk} \gg H_{\text{ank}}$ , the states  $(\mathbf{m}_1, \mathbf{m}_2) = (\mathbf{e}_z, \mathbf{e}_z)$  and  $(-\mathbf{e}_z, -\mathbf{e}_z)$  correspond to the energy minima.

The purpose of this paper is to investigate the switching rate of the magnetizations  $\mathbf{m}_1$  and  $\mathbf{m}_2$  from  $\mathbf{m}_1, \mathbf{m}_2 =$

$+\mathbf{e}_z$  to  $\mathbf{m}_1, \mathbf{m}_2 = -\mathbf{e}_z$ . Following Brown<sup>14</sup>, we use the Fokker-Planck equation approach to calculate the switching probability per unit time, where the Fokker-Planck equation is derived from the equations of the motion of the magnetizations.

We assume that the dynamics of the magnetizations of the  $F_1$  and  $F_2$  layers are described by the Landau-Lifshitz-Gilbert (LLG) equations. In general, the spin transfer torque acting on  $\mathbf{m}_1$  arises from the spin currents injected from the fixed layer and the  $F_2$  layer. However, in a conventional synthetic free layer, the spacer layer between the  $F_1$  and  $F_2$  layers consists of Ru, whose spin diffusion length is comparable to its thickness<sup>15</sup>; thus, the spin current injected from the  $F_2$  layer is negligible<sup>16</sup>. Then, the LLG equation of  $\mathbf{m}_1$  is given by

$$\begin{aligned}
 \frac{d\mathbf{m}_1}{dt} = & -\gamma_1 \mathbf{m}_1 \times \mathbf{H}_1 + \gamma_1 a_J \mathbf{m}_1 \times (\mathbf{p} \times \mathbf{m}_1) \\
 & -\gamma_1 \mathbf{m}_1 \times \mathbf{h}_1 + \alpha_1 \mathbf{m}_1 \times \frac{d\mathbf{m}_1}{dt}. \quad (2)
 \end{aligned}$$

Similarly, the spin current injected from the  $F_1$  layer into the  $F_2$  layer is also negligible, and the LLG equation of  $\mathbf{m}_2$  is given by

$$\frac{d\mathbf{m}_2}{dt} = -\gamma_2 \mathbf{m}_2 \times \mathbf{H}_2 - \gamma_2 \mathbf{m}_2 \times \mathbf{h}_2 + \alpha_2 \mathbf{m}_2 \times \frac{d\mathbf{m}_2}{dt}, \quad (3)$$

where  $\gamma_k$  and  $\alpha_k$  are the gyromagnetic ratio and the Gilbert damping constant of the  $F_k$  layer, respectively. The magnetic field  $\mathbf{H}_k$  acting on the magnetization  $\mathbf{m}_k$  is defined by  $\mathbf{H}_k = -(M_k V_k)^{-1} \partial F / \partial \mathbf{m}_k$ .  $\mathbf{h}_k$  represents the random field on the  $F_k$  layer whose Cartesian components  $h_{ki}$  ( $i = x, y, z$ ) satisfy

$$\langle h_{ki}(t) h_{k'j}(t') \rangle = \frac{2k_B T \alpha_k}{\gamma_k M_k V_k} \delta_{kk'} \delta_{ij} \delta(t - t'), \quad (4)$$

where  $\langle \dots \rangle$  means the ensemble average. Here we assume no correlation between the random fields acting on the  $F_1$  and  $F_2$  layers. The  $a_J = \hbar \eta I / (2e M_1 V_1)$  term in Eq. (2) represents the spin transfer torque due to the injection of the spin current from the fixed layer. Here  $I$  is the electric current flowing along the  $x$  axis. The positive electric current corresponds to the electron flow along the  $-x$  direction.  $\eta$  is the spin polarization of the electric current which characterizes the strength of the spin transfer torque. The explicit form of  $\eta$  depends on the theoretical model<sup>1,17,18</sup>, and, in general, depends on  $\theta_1$ . However, for simplicity, we assume that  $\eta$  is constant (the dependence of  $\eta$  on  $\theta_1$  can be taken into account by replacing  $a_J \cos \theta_1$  in Eq. (6) with  $\int d \cos \theta_1 a_J$ ).  $\mathbf{p}$  is the unit vector along the direction of the magnetization of the fixed layer.

From the LLG equations (2) and (3), we obtain the Fokker-Planck equation for the probability distribution of the directions of the magnetizations,  $W(\mathbf{m}_1, \mathbf{m}_2)$ ,

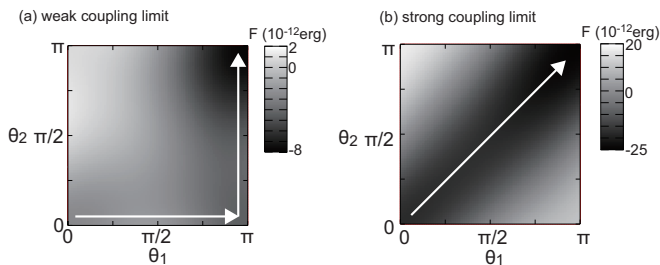


FIG. 2: The dependences of the effective potential  $\mathcal{F}(\theta_1, \theta_2)$  on  $\theta_1$  and  $\theta_2$  for (a) the weak coupling limit and (b) the strong coupling limit. The values of the parameters are written in Secs. III and IV. The white arrows indicate the most probable paths of the switchings  $\mathbf{m}_1, \mathbf{m}_2 = +\mathbf{e}_z \rightarrow -\mathbf{e}_z$ .

which is given by<sup>14</sup>

$$\begin{aligned}
\frac{\partial W}{\partial t} = & \frac{\gamma_1}{M_1 V_1} \frac{1}{\sin \theta_1} \frac{\partial}{\partial \theta_1} \\
& \left[ \sin \theta_1 \left\{ \left( \alpha_1 \frac{\partial F}{\partial \theta_1} + \frac{1}{\sin \theta_1} \frac{\partial F}{\partial \varphi_1} + a_J M_1 V_1 \sin \theta_1 \right) W \right. \right. \\
& \quad \left. \left. + \alpha_1 k_B T \frac{\partial W}{\partial \theta_1} \right\} \right] \\
& + \frac{\gamma_1}{M_1 V_1} \frac{1}{\sin \theta_1} \frac{\partial}{\partial \varphi_1} \\
& \left[ \left( \frac{\alpha_1}{\sin \theta_1} \frac{\partial F}{\partial \varphi_1} - \frac{\partial F}{\partial \theta_1} \right) W + \frac{\alpha_1 k_B T}{\sin \theta_1} \frac{\partial W}{\partial \varphi_1} \right] \\
& + \frac{\gamma_2}{M_2 V_2} \frac{1}{\sin \theta_2} \frac{\partial}{\partial \theta_2} \\
& \left[ \sin \theta_2 \left\{ \left( \alpha_2 \frac{\partial F}{\partial \theta_2} + \frac{1}{\sin \theta_2} \frac{\partial F}{\partial \varphi_2} \right) W + \alpha_2 k_B T \frac{\partial W}{\partial \theta_2} \right\} \right] \\
& + \frac{\gamma_2}{M_2 V_2} \frac{1}{\sin \theta_2} \frac{\partial}{\partial \varphi_2} \\
& \left[ \left( \frac{\alpha_2}{\sin \theta_2} \frac{\partial F}{\partial \varphi_2} - \frac{\partial F}{\partial \theta_2} \right) W + \frac{\alpha_2 k_B T}{\sin \theta_2} \frac{\partial W}{\partial \varphi_2} \right]. \tag{5}
\end{aligned}$$

Here we approximate that  $1 + \alpha_k^2 \simeq 1$  by assuming that  $\alpha_k \ll 1$ <sup>19</sup>. We also neglect the term proportional to  $\alpha a_J$  by assuming that  $|a_J| < |\mathbf{H}_k|$ , which is valid in the thermally assisted switching region.

As shown by Brown<sup>14</sup>, the switching rate of the single ferromagnetic layer without spin transfer torque can be derived by using the steady-state solution of the Fokker-Planck equation and the continuity equation of the particles of an ensemble [see Sec. 4. C in Ref.<sup>14</sup>]. In the case of two ferromagnetic layers, as considered in this paper, the switching is described by the particle flow in  $(\theta_1, \varphi_1, \theta_2, \varphi_2)$  four-dimensional phase space, and, in general, it is very difficult to obtain an analytical expression of the switching rate because the particle flow in the phase space is very complicated. To simplify the problem, we use the following two approximations.

First, we assume that the magnetization rotates in the  $yz$  plane during the switching. Since the deviation of the

magnetization  $\mathbf{m}_k$  from the  $yz$  plane increases the magnetic energy due to the demagnetization field, it is reasonable to assume that the most probable reversal process is the magnetization reversal in the  $yz$  plane. In this limit, the demagnetization field plays no role on the calculation of the switching probability. By fixing the values of  $\varphi_1$  and  $\varphi_2$  to  $\pi/2$  or  $3\pi/2$ , the steady-state solution of the Fokker-Planck equation (5) is given by  $W_0 \propto \exp[-\mathcal{F}/(k_B T)]$ , where the effective free energy  $\mathcal{F}$  is given by

$$\mathcal{F} = F - \frac{a_J M_1 V_1}{\alpha_1} \cos \theta_1. \tag{6}$$

The switching probability is calculated by using  $W_0 \propto \exp[-\mathcal{F}/(k_B T)]$ .

The second approximation is that we consider the switching for the weak and strong coupling limits, where the weak (strong) coupling means that the magnitude of the coupling energy of the  $F_1$  and  $F_2$  layers,  $| -J S \mathbf{m}_1 \cdot \mathbf{m}_2 |$ , is much smaller (larger) than the uniaxial anisotropy energy  $M_k H_{\text{ank}} V_k / 2$ . In other words, the weak (strong) coupling limit corresponds to  $H_{\text{ank}} \gg (\ll) H_{Jk}$ . The weak and strong coupling limit can be realized by changing the thickness of the nonmagnetic layer  $d_N$  between  $F_1$  and  $F_2$  layers because the magnitude of the coupling constant  $J$  strongly depends on  $d_N$  [see, for example, Fig. 2 in Ref.<sup>8</sup> or Fig. 1 (c) in Ref.<sup>10</sup>], and varies from  $H_J \sim 1 \times 10^3$  Oe to 1 Oe or less. Figures 2 (a) and (b) show the dependences of  $\mathcal{F}$  on  $(\theta_1, \theta_2)$  for the weak and the strong coupling limit, respectively, where the white arrows indicate the most probable paths of the switching (the values of the parameters are written in Secs. III and IV with  $a_J/a_{c1} = 0.5$ ). In the weak coupling limit, the magnetization reversal is divided into two steps: First  $\mathbf{m}_1$  reverses its direction from  $\mathbf{m}_1 = +\mathbf{e}_z$  to  $\mathbf{m}_2 = -\mathbf{e}_z$  by the thermally assisted spin transfer torque effect while the direction of  $\mathbf{m}_2$  is fixed to  $\mathbf{m}_2 = +\mathbf{e}_z$ , and second,  $\mathbf{m}_2$  reverses its direction by the thermal effect and the coupling with the  $F_1$  layer while  $\mathbf{m}_1$  is fixed to  $\mathbf{m}_1 = -\mathbf{e}_z$ . On the other hand, in the strong coupling limit,  $\mathbf{m}_1$  and  $\mathbf{m}_2$  reverse their directions simultaneously.

By using the above two approximations, the calculation of the switching rate is reduced to a one-dimensional problem. For the weak coupling limit, first we calculate the particle flow in  $\theta_1$  space, and second, we calculate the particle flow in  $\theta_2$  space. On the other hand, for the strong coupling limit, we calculate the particle flow along the direction of  $\theta_1 = \theta_2$ . For such one dimensional problems, the calculation method developed by Brown<sup>14</sup> is applicable to obtain the switching rate with some revisions. In Secs. III and IV, we show the switching probabilities for the weak and strong coupling limit, respectively.

At the end of this section, we give a brief comment on the first approximation. The influence of the first approximation is that the critical current density estimated in our calculation,  $I_c \propto (H_{\text{appl}} + H_{\text{an}})$ , does not include the effect of the demagnetization field  $4\pi M$  [see Eqs. (15), (16), (22) and (23)] while the critical current density esti-

mated by the LLG equation includes the demagnetization field, that is,  $I_c \propto (H_{\text{appl}} + H_{\text{an}} + 2\pi M)$  [see, for example, Eq. (14) in Ref.<sup>12</sup>]. Since  $4\pi M \gg |H_{\text{appl}}|, H_{\text{an}}$ , the critical current density in our formula ( $10^{5-6}$  A/cm<sup>2</sup>) is much smaller than the experimental values ( $10^{6-7}$  A/cm<sup>2</sup>)<sup>8-10</sup>. One way to solve this discrepancy is as follows. Although we consider the in-plane magnetized system, it should be noted that our calculation is directly applicable to the perpendicularly magnetized system where the system has uni-axial symmetry and the switchings in the weak and strong coupling limits are described by only  $\theta_1$  and  $\theta_2$ . Suzuki *et al.*<sup>20</sup> showed that the effect of the demagnetization field on the switching rate of the in-plane magnetized system can be taken into account by replacing  $H_{\text{an}}$  in the switching formula of the perpendicularly magnetized system by  $H_{\text{an}} + 2\pi M$ . By applying this replacement to our formula, our formula may be applicable to analyze the experiments quantitatively. The validity of this replacement requires the numerical calculation of the Fokker-Planck equation, and it is beyond the scope of this paper.

### III. WEAK COUPLING LIMIT

In this section, we derive the switching rate of the magnetizations for the weak coupling limit ( $H_{\text{ank}} \gg H_{Jk}$ ) [see also the Appendix]. With this limit, the magnetization reversal is divided into two steps, as mentioned in Sec. II. For convenience, we label the three regions around the potential minimum in the phase space,  $(\theta_1, \theta_2) = (0, 0), (\pi, 0)$ , and  $(\pi, \pi)$ , as regions 1, 2, and 3, respectively. The first step ( $\mathbf{m}_1$  reverses from  $+\mathbf{e}_z$  to  $-\mathbf{e}_z$ ) corresponds to the transition of the particle from region 1 to region 2 while the second step ( $\mathbf{m}_2$  reverses from  $+\mathbf{e}_z$  to  $-\mathbf{e}_z$ ) corresponds to the transition from region 2 to region 3.

The switching rate from region 1 to region 2 is obtained as follows<sup>14</sup>. In regions 1 and 2, the distribution  $W(\theta_1, \theta_2)$  is given by  $W_1 \exp[-\{\mathcal{F}(\theta_1, 0) - \mathcal{F}(0, 0)\}/(k_B T)]$  and  $W_2 \exp[-\{\mathcal{F}(\theta_1, 0) - \mathcal{F}(\pi, 0)\}/(k_B T)]$ , respectively, where  $W_1 = W(0, 0)$  and  $W_2 = W(\pi, 0)$ . The numbers of particles in region 1,  $n_1$ , is obtained by integrating  $W(\theta_1, 0)$  over  $[0, \theta_{m1}]$ , where  $\theta_{m1} = \cos^{-1}[-(H_{\text{appl}} + H_{J1} + a_J/\alpha_1)/H_{\text{an}1}]$  gives the local maximum of the effective potential  $\mathcal{F}(\theta_1, 0)$ . The explicit form of  $n_1$  is given by  $n_1 = 2W_1 e^{\mathcal{F}(0, 0)/(k_B T)} I_1$ , where factor 2 arises from the fact that we restrict the particle flow in the  $yz$  plane; that is,  $\varphi_1 = \pi/2$  or  $3\pi/2$  (in the anisotropic system considered by Brown<sup>14</sup>, the numerical factor is  $2\pi$ , not 2, as shown in Eq. (4.26) of Ref.<sup>14</sup>). The integral  $I_1 = \int_0^{\theta_{m1}} d\theta_1 \sin \theta_1 \exp[-\mathcal{F}(\theta_1, 0)/(k_B T)]$  can be

approximated to<sup>14</sup>

$$\begin{aligned} I_1 &\simeq e^{-\mathcal{F}(0, 0)/(k_B T)} \int_0^\infty d\theta_1 \theta_1 \exp \left[ -\frac{1}{2k_B T} \frac{\partial^2 \mathcal{F}(\theta_1, 0)}{\partial \theta_1^2} \theta_1^2 \right] \\ &= e^{-\mathcal{F}(0, 0)/(k_B T)} \frac{k_B T}{\partial^2 \mathcal{F}(0, 0)/\partial \theta_1^2}. \end{aligned} \quad (7)$$

The numbers of particle in region 2,  $n_2 = 2W_2 e^{\mathcal{F}(\pi, 0)/(k_B T)} I_2$ , is obtained in a similar way by replacing the factors  $\mathcal{F}(0, 0)$  and  $\partial^2 \mathcal{F}(0, 0)/\partial \theta_1^2$  to  $\mathcal{F}(\pi, 0)$  and  $\partial^2 \mathcal{F}(\pi, 0)/\partial \theta_1^2$ , respectively. Next, we consider the particle flow from region 1 to region 2,  $I_{1 \rightarrow 2}$ . From the Fokker-Planck equation (5), the particle flow along the  $\theta_1$ -axis,  $J_{\theta_1}$ , which satisfies  $I_{1 \rightarrow 2} = 2 \sin \theta_1 J_{\theta_1}$ , is identified as

$$J_{\theta_1} = -\frac{\alpha_1 \gamma_1}{M_1 V_1} \left[ \left( \frac{\partial F}{\partial \theta_1} + \frac{a_J M_1 V_1}{\alpha_1} \sin \theta_1 \right) W + k_B T \frac{\partial W}{\partial \theta_1} \right]. \quad (8)$$

By multiplying  $e^{\mathcal{F}(\theta_1, 0)/(k_B T)}$  to  $I_{1 \rightarrow 2}/(2 \sin \theta_1) = J_{\theta_1}$  and integrating it over  $[0, \pi]$ , we find that  $[(n_2/I_2) - (n_1/I_1)]/2 = -[M_1 V_1/(2\alpha_1 \gamma_1 k_B T)] I_{1 \rightarrow 2} I_{m1}$ , where the integral  $I_{m1} = \int_0^\pi d\theta_1 e^{\mathcal{F}(\theta_1, 0)/(k_B T)}/\sin \theta_1$  can be approximated to<sup>14</sup>

$$\begin{aligned} I_{m1} &\simeq \frac{e^{\mathcal{F}(\theta_{m1}, 0)/(k_B T)}}{\sin \theta_{m1}} \\ &\quad \times \int_{-\infty}^\infty d\theta_1 \exp \left[ \frac{(\theta_1 - \theta_{m1})^2}{2k_B T} \frac{\partial^2 \mathcal{F}(\theta_{m1}, 0)}{\partial \theta_1^2} \right] \\ &= \sqrt{\frac{2\pi k_B T}{\partial^2 \mathcal{F}(\theta_{m1}, 0)/\partial \theta_1^2}} \frac{e^{\mathcal{F}(\theta_{m1}, 0)/(k_B T)}}{\sin \theta_{m1}}. \end{aligned} \quad (9)$$

The relation between the particle numbers in region 2 and 3,  $n_2$  and  $n_3$ , and the particle flow from region 2 to region 3,  $I_{2 \rightarrow 3}$ , is obtained in a similar way. Then, by using the continuity equations of the particle flow,  $\dot{n}_1 = -I_{1 \rightarrow 2}$ ,  $\dot{n}_2 = I_{1 \rightarrow 2} - I_{2 \rightarrow 3}$ , and  $\dot{n}_3 = I_{2 \rightarrow 3}$ , we find that the transitions of the magnetization directions among the three states,  $(\theta_1, \theta_2) = (0, 0), (\pi, 0), (\pi, \pi)$ , are described by the following differential equations:

$$\frac{d}{dt} \begin{pmatrix} n_1 \\ n_2 \\ n_3 \end{pmatrix} = \begin{pmatrix} -\nu_{12} & \nu_{21} & 0 \\ \nu_{12} & -(\nu_{21} + \nu_{23}) & \nu_{32} \\ 0 & \nu_{23} & -\nu_{32} \end{pmatrix} \begin{pmatrix} n_1 \\ n_2 \\ n_3 \end{pmatrix}. \quad (10)$$

The switching probability per unit time from the region  $i$  to the region  $j$  is given by  $\nu_{ij} = f_{ij} \exp(-\Delta_{ij})$ , where the attempt frequency  $f_{ij}$  and the thermal stability  $\Delta_{ij}$  are, respectively, given by

$$\begin{aligned} f_{12(21)} &= \left( \frac{\alpha_1 \gamma_1 k_B T}{M_1 V_1} \right) \frac{M_1 H_{\text{an}1} V_1}{k_B T} \sqrt{\frac{M_1 H_{\text{an}1} V_1}{2\pi k_B T}} \\ &\quad \times \left( 1 + (-) \frac{H_{\text{appl}} + H_{J1}}{H_{\text{an}1}} \right) \left( 1 - \frac{I}{I_{c1(2)}} \right) \\ &\quad \times \left[ 1 - \left( \frac{H_{\text{appl}} + H_{J1}}{H_{\text{an}1}} \right)^2 \right] \left( 1 - \frac{I}{I_{c1}} \right) \left( 1 - \frac{I}{I_{c2}} \right), \end{aligned} \quad (11)$$

$$\Delta_{12(21)} = \frac{M_1 H_{\text{an}1} V_1}{2k_B T} \left( 1 + (-) \frac{H_{\text{appl}} + H_{J1}}{H_{\text{an}1}} \right)^2 \times \left( 1 - \frac{I}{I_{c1(2)}} \right)^2, \quad (12)$$

$$f_{23(32)} = \left( \frac{\alpha_2 \gamma_2 k_B T}{M_2 V_2} \right) \frac{M_2 H_{\text{an}2} V_2}{k_B T} \sqrt{\frac{M_2 H_{\text{an}2} V_2}{2\pi k_B T}} \times \left( 1 + (-) \frac{H_{\text{appl}} - H_{J2}}{H_{\text{an}2}} \right) \times \left[ 1 - \left( \frac{H_{\text{appl}} - H_{J2}}{H_{\text{an}2}} \right)^2 \right], \quad (13)$$

$$\Delta_{23(32)} = \frac{M_2 H_{\text{an}2} V_2}{2k_B T} \left( 1 + (-) \frac{H_{\text{appl}} - H_{J2}}{H_{\text{an}2}} \right)^2. \quad (14)$$

Here  $I/I_{c1} = a_J/a_{c1}$  and  $I/I_{c2} = a_J/a_{c2}$ .  $a_{c1}$  ( $a_{c2}$ ) is the critical spin-transfer torque field to induce the magnetization reversal from region 1 (2) to region 2 (1) at zero temperature, and their explicit forms are given by

$$a_{c1} = -\alpha_1 (H_{\text{appl}} + H_{J1} + H_{\text{an}1}), \quad (15)$$

$$a_{c2} = \alpha_1 (-H_{\text{appl}} - H_{J1} + H_{\text{an}1}), \quad (16)$$

respectively. Since  $|H_{\text{appl}} + H_{J1}|$  is assumed to be smaller than  $H_{\text{an}1}$ , we find that  $a_{c1} < 0$  and  $a_{c2} > 0$ . It should be noted that the description of the transition of the magnetization by Eq. (10) is valid for  $|a_J| < |a_{ck}|$  because if  $|a_J| \gg |a_{ck}|$ , the point  $\mathbf{m}_1 = +\mathbf{e}_z$  ( $-\mathbf{e}_z$ ) would be unstable, and then we could not discuss the thermally assisted transition. We also note that the switching probabilities of  $\mathbf{m}_2$ ,  $\nu_{23}$  and  $\nu_{32}$ , are reduced to those obtained by Brown<sup>14</sup> by omitting  $H_{J2}$  where  $\nu_{23}$  and  $\nu_{32}$  are independent of the current  $I$ .

When  $I$  is nearly  $I_{c1}$ , we find that  $\nu_{12}/\nu_{21} \sim \exp[M_1 H_{\text{an}1} V_1 / (2k_B T)] \gg 1$ . Similarly, when  $-H_{\text{appl}} + H_{J2} > 0$ , we find that  $\nu_{23}/\nu_{32} \sim \exp[2M_2 (-H_{\text{appl}} + H_{J2}) V_2 / (2k_B T)] \gg 1$ . Within these limits, the analytical solutions of Eq. (10) with the initial conditions  $n_1(0) = 1$ ,  $n_2(0) = 0$ , and  $n_3(0) = 0$ , are given by

$$n_1(t) = e^{-\nu_{12}t}, \quad (17)$$

$$n_2(t) = -\frac{\nu_{12}}{\nu_{12} - \nu_{23}} (e^{-\nu_{12}t} - e^{-\nu_{23}t}), \quad (18)$$

$$n_3(t) = 1 - \frac{\nu_{12}e^{-\nu_{23}t} - \nu_{23}e^{-\nu_{12}t}}{\nu_{12} - \nu_{23}}. \quad (19)$$

Equation (19) is the central result of this section: It completely describes the magnetization switching of the synthetic free layer within the weak coupling limit.

Figure 3 (a) shows a typical time evolution of  $n_1(t)$ ,  $n_2(t)$ , and  $n_3(t)$  for a synthetic free layer with  $M = 995$

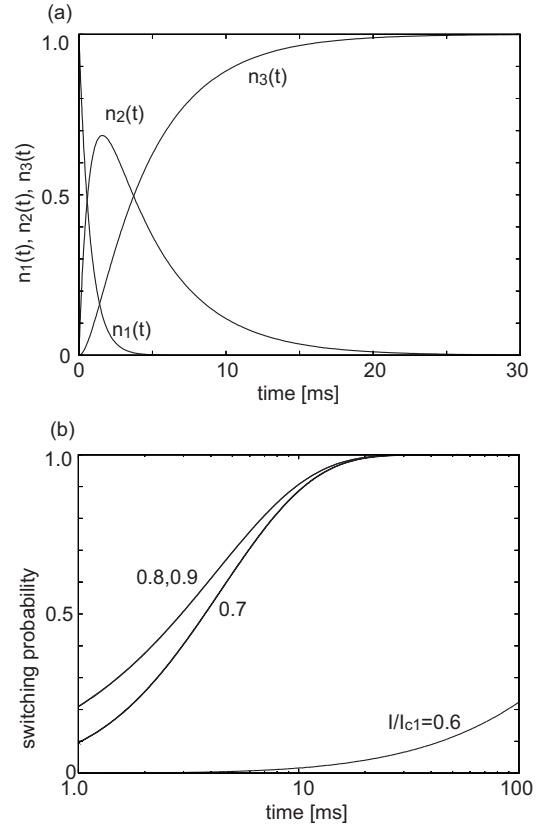


FIG. 3: (a) Time evolution of  $n_1(t)$ ,  $n_2(t)$ , and  $n_3(t)$  with  $I/I_{c1} = 0.7$  for the weak coupling limit. (b) The dependence of the switching rate  $n_3(t)$  on the ratio  $I/I_{c1}$  for the weak coupling limit. For  $I/I_{c1} \geq 0.8$ , the switching time is saturated. The horizontal axis is the logarithmic scale.

emu/c.c.,  $H_{\text{an}} = 50$  Oe,  $H_{\text{appl}} = 0$  Oe,  $\alpha = 0.007$ ,  $\gamma = 1.732 \times 10^7$  Hz/Oe,  $d = 2$  nm,  $S = \pi \times 70 \times 160$  nm<sup>2</sup>, and  $T = 300$  K (for simplicity, we assume that  $F_1 = F_2$ )<sup>9,10,21</sup>. The current is taken to be  $I/I_{c1} = 0.7$ . The coupling constant is assumed to be  $J = 5.0 \times 10^{-3}$  erg/cm<sup>2</sup>, which corresponds to  $H_J = 25$  Oe. From Eqs. (17), (18) and (19), one can easily see that the time evolution shown in Fig. 3 (a) is determined by two time scales,  $\nu_{12}^{-1}$  and  $\nu_{23}^{-1}$ , which correspond to the switching rates of the  $F_1$  and  $F_2$  layers, respectively. Figure 3 (b) shows the dependence of the switching rate  $n_3(t)$  on the ratio  $I/I_{c1}$ . For the currents  $|I| \geq 0.7|I_{c1}|$ , the switching times are on the same order (10 ms for our parameters), and for the large currents  $|I| \geq 0.8|I_{c1}|$ , the switching times are saturated. This is because the current determines the switching time of the  $F_1$  layer only, and for a large current, the total switching time of  $\mathbf{m}_1$  and  $\mathbf{m}_2$  is mainly determined by the switching time of  $\mathbf{m}_2$ , which is independent of the current. We can verify the saturation of the switching time from Eq. (19), where  $\nu_{12}$  becomes much larger than  $\nu_{23}$  as  $I$  approaches  $I_{c1}$  and then,  $n_3(t) \simeq 1 - e^{-\nu_{23}t}$ , which is independent of the current  $I$ . On the other hand, in the low current region  $|I| \ll |I_{c1}|$ ,  $\nu_{12}$  becomes comparable or smaller than  $\nu_{23}$ , which leads

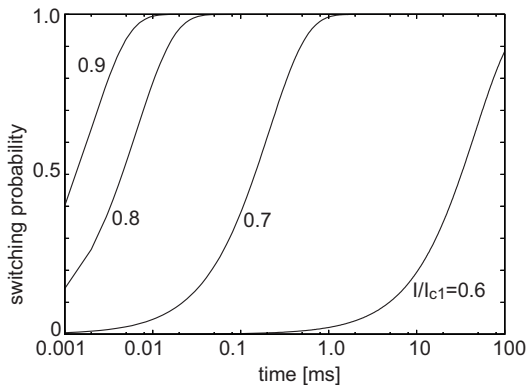


FIG. 4: The dependence of the switching rate  $n_2(t)$  on the ratio  $I/I_{c1}$  for the strong coupling limit. The horizontal axis is the logarithmic scale.

to  $n_3(t) \simeq 1 - e^{-\nu_{12}t}$ . Then the switching time strongly depends on the current value because the switching time of  $\mathbf{m}_1$  becomes important to the total switching time. For example, the switching time for  $I/I_{c1} = 0.6$  is longer than 100 ms, as shown in Fig. 3 (b).

The dependence of the switching time on the coupling constant  $J$  is as follow. By increasing the magnitude of  $H_J$ , the switching time rapidly decreases because of the fast reversal of the magnetization of the  $F_2$  layer. For example, for  $H_J = 40$  Oe with  $I/I_c = 0.9$ , the switching time is on the order of  $10^{-2}$  ms, which is three orders of magnitude faster than that for  $H_J = 25$  Oe. On the other hand, by decreasing the magnitude of  $H_J$ , only the magnetization of the  $F_1$  layer reverses its direction while the magnetization of the  $F_2$  layer remains  $\mathbf{m}_2 = +\mathbf{e}_z$ . For example, for  $H_J = 5$  Oe with  $I/I_c = 0.9$ , the switching time of the  $F_1$  layer is on the order of  $10^{-2}$  ms while the switching rate of the  $F_2$  layer,  $n_3$ , is approximately zero ( $n_3 \sim 10^{-9}$ ). Since the switching of the  $F_2$  layer is induced by the coupling with the  $F_1$  layer, it is required to increase the magnitude of the coupling constant  $J$  for the fast switching by using a thin nonmagnetic spacer, although the increase of the coupling constant leads to the increase of the magnitude of the critical current density.

#### IV. STRONG COUPLING LIMIT

In this section, we derive the switching rate of the magnetizations for the strong coupling limit ( $H_{\text{ank}} \ll H_{Jk}$ ). For this limit, instead of  $(\theta_1, \theta_2)$  phase space, it is convenient to describe the particle flow in  $(\Psi, \psi)$  phase space, where  $\Psi = (\theta_1 + \theta_2)/2$  and  $\psi = \theta_1 - \theta_2$ . Since  $\mathbf{m}_1$  and  $\mathbf{m}_2$  reverse their directions simultaneously, the reversal is described by the particle flow along the  $\Psi$ -axis with  $\psi = 0$ . For convenience, we label the two regions around the potential minimum in the phase space,  $(\Psi, \psi) = (0, 0)$  and  $(\pi, 0)$ , as regions 1 and 2, respectively. The continuity equation of the particle in the regions 1 and 2 is obtained in a way similar to that described in Sec. III

and is expressed as  $\dot{n}_1 = -\dot{n}_2 = -\nu_{12}n_1 + \nu_{21}n_2$ . The switching probability  $\nu_{ij} = f_{ij} \exp(-\Delta_{ij})$  is given by

$$f_{12(21)} = \frac{k_B T}{2} \left( \frac{\alpha_1 \gamma_1}{M_1 V_1} + \frac{\alpha_2 \gamma_2}{M_2 V_2} \right) \frac{M_1 H_{\text{an1}} V_1 + M_2 H_{\text{an2}} V_2}{k_B T} \times \sqrt{\frac{M_1 H_{\text{an1}} V_1 + M_2 H_{\text{an2}} V_2}{2\pi k_B T}} \times \left( 1 + (-) \frac{M_1 H_{\text{appl}} V_1 + M_2 H_{\text{appl}} V_2}{M_1 H_{\text{an1}} V_1 + M_2 H_{\text{an2}} V_2} \right) \left( 1 - \frac{I}{I_{c1(2)}} \right) \times \left[ 1 - \left( \frac{M_1 H_{\text{appl}} V_1 + M_2 H_{\text{appl}} V_2}{M_1 H_{\text{an1}} V_1 + M_2 H_{\text{an2}} V_2} \right)^2 \right] \times \left( 1 - \frac{I}{I_{c1}} \right) \left( 1 - \frac{I}{I_{c2}} \right), \quad (20)$$

$$\Delta_{12(21)} = \frac{M_1 H_{\text{an1}} V_1 + M_2 H_{\text{an2}} V_2}{2k_B T} \times \left( 1 + (-) \frac{M_1 H_{\text{appl}} V_1 + M_2 H_{\text{appl}} V_2}{M_1 H_{\text{an1}} V_1 + M_2 H_{\text{an2}} V_2} \right)^2 \times \left( 1 - \frac{I}{I_{c1(2)}} \right)^2, \quad (21)$$

where  $I/I_{c1} = a_J/a_{c1}$  and  $I/I_{c2} = a_J/a_{c2}$ , and the critical spin-transfer torque fields in the strong coupling limit  $a_{ck}$  are given by

$$a_{c1} = -\alpha_1 \left[ H_{\text{appl}} + H_{\text{an1}} + \frac{M_2 V_2}{M_1 V_1} (H_{\text{appl}} + H_{\text{an2}}) \right], \quad (22)$$

$$a_{c2} = \alpha_1 \left[ -H_{\text{appl}} + H_{\text{an1}} + \frac{M_2 V_2}{M_1 V_1} (-H_{\text{appl}} + H_{\text{an2}}) \right], \quad (23)$$

respectively. The analytical solutions of the transition equations,  $\dot{n}_1 = -\dot{n}_2 = -\nu_{12}n_1 + \nu_{21}n_2$ , with the initial conditions  $n_1(0) = 1$  and  $n_2(0) = 0$  are given by

$$n_1(t) = \frac{\nu_{21}}{\nu_{12} + \nu_{21}} + \frac{\nu_{12}}{\nu_{12} + \nu_{21}} e^{-(\nu_{12} + \nu_{21})t}, \quad (24)$$

$$n_2(t) = \frac{\nu_{12}}{\nu_{12} + \nu_{21}} - \frac{\nu_{12}}{\nu_{12} + \nu_{21}} e^{-(\nu_{12} + \nu_{21})t}. \quad (25)$$

When  $I$  is nearly  $I_{c1}$ ,  $\nu_{12}/\nu_{21} \sim \exp[(M_1 H_{\text{an1}} V_1 + M_2 H_{\text{an2}} V_2)/(2k_B T)] \gg 1$ . For this limit, Eqs. (24) and (25) are reduced to

$$n_1(t) \simeq e^{-\nu_{12}t}, \quad (26)$$

$$n_2(t) \simeq 1 - e^{-\nu_{12}t}. \quad (27)$$

Equation (27) is the central result of this section: It completely describes the magnetization switching of the synthetic free layer within the strong coupling limit.



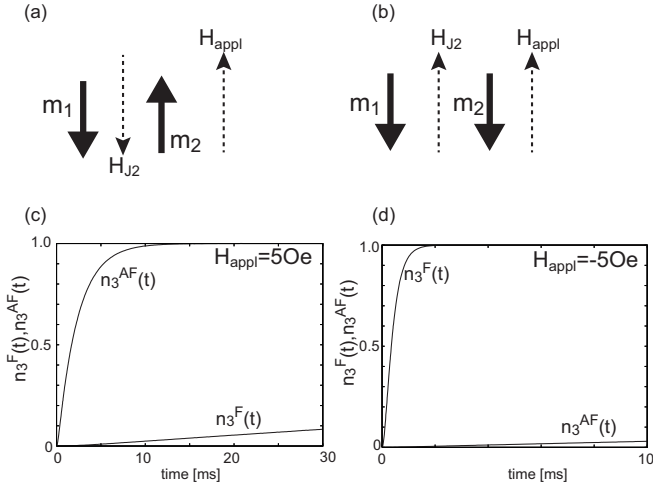


FIG. 5: (a), (b): The schematic views of the alignments of the magnetizations  $\mathbf{m}_1$  and  $\mathbf{m}_2$  of (a) ferromagnetically (F) coupled and (b) anti-ferromagnetically (AF) coupled synthetic free layers after  $\mathbf{m}_1$  reverses its direction from the initial state ( $\mathbf{m}_1 = +\mathbf{e}_z$ ) to  $\mathbf{m}_1 = -\mathbf{e}_z$ . The directions of the applied field  $H_{\text{appl}}$  (assumed to be positive) and the coupling field  $H_{J2}$  are also denoted. (c), (d): The time evolution of  $n_3(t)$  of the F-coupled ( $n_3^{(F)}(t)$ ) and the AF-coupled ( $n_3^{(AF)}(t)$ ) synthetic free layer with (c)  $H_{\text{appl}} = +5$  Oe and (d)  $H_{\text{appl}} = -5$  Oe. The value of the current is taken to be  $I/I_{c1} = 0.7$ .

For the strong coupling limit, the switching time strongly depends on the current  $I$  for all current region. Figure 4 shows the dependence of  $n_2(t)$  on the ratio  $I/I_{c1}$ , where the parameters used are same as those in Fig. 3 except  $J$ . The coupling constant  $J$  is assumed to be  $5.0 \times 10^{-2}$  erg/cm $^{-2}$ , which corresponds to  $H_J = 250$  Oe. The orders of the switching times are  $10^{-2}$  ms for  $I/I_{c1} = 0.8, 0.9$ , 1 ms for  $I/I_{c1} = 0.7$ , and more than 100 ms for  $I/I_{c1} \leq 0.6$  in our parameter region, as shown in Fig. 4. Such strong dependence of the switching time on the current arises from the thermal stability  $\Delta_{12}$ , which is proportional to  $(1 - I/I_{c1})^2$ , as shown in Eq. (21).

## V. RELATION TO OTHER WORKS

In this section, we compare the results obtained in the previous sections to the other works<sup>8-11</sup>. The topics discussed here are (1) the comparison of the switching time of the ferromagnetically (F) and the anti-ferromagnetically (AF) coupled synthetic free layers, and (2) the comparison of the dependence of the thermal stability to that obtained by Koch *et al.*<sup>11</sup>.

First, we discuss the switching times of the F and the AF-coupled synthetic free layers. The difference in the switching times of these two kinds of synthetic free layer appears in the weak coupling limit with finite  $H_{\text{appl}}$ . In this case, the switching time of the F-coupled synthetic free layer is characterized by Eqs. (12) and (14). For the AF-coupled synthetic free layer, the fac-

tor  $+(-)(H_{\text{appl}} - H_{J2})/H_{\text{an}2}$  in Eq. (14) is replaced by  $-(+)(H_{\text{appl}} + H_{J2})/H_{\text{an}2}$  while Eq. (12) remains the same. This replacement is due to the fact that after  $\mathbf{m}_1$  reverses its direction from  $+\mathbf{e}_z$  to  $-\mathbf{e}_z$ , the sum of the applied field  $H_{\text{appl}}$  and the coupling field  $H_{J2}$  acting on  $\mathbf{m}_2$  is  $H_{\text{appl}} - H_{J2}$  for the F-coupled synthetic free layer while it is  $H_{\text{appl}} + H_{J2}$  for the AF-coupled synthetic free layer, as schematically shown in Figs. 5 (a) and (b), and leads to the difference in the switching times of the F-coupled and the AF-coupled synthetic layers.

The important point is that the fast switching is achieved by choosing the appropriate direction of  $H_{\text{appl}}$ . Figures 5 (c) and (d) show the time evolutions of  $n_3(t)$  (Eq. (19)) for the F-coupled ( $n_3^{(F)}$ ) and the AF-coupled ( $n_3^{(AF)}$ ) synthetic free layers with (c)  $H_{\text{appl}} = +5$  Oe and (d)  $H_{\text{appl}} = -5$  Oe. The current is taken to be  $I/I_{c1} = 0.7$ . The switching time of the AF (F) coupled synthetic free layer is faster compared to that of the F (AF) coupled synthetic free layer for  $H_{\text{appl}} > 0 (< 0)$  because both  $H_{\text{appl}}$  and  $H_{J2}$  assist the reversal of  $\mathbf{m}_2$ . On the other hand, by changing the direction (sign) of  $H_{\text{appl}}$ , the switching time increases significantly because of the exponential dependence of the switching time ( $\sim 1/\nu$ ) on  $\Delta \propto [1 - (H_{\text{appl}} \pm H_J)/H_{\text{an}}]^2$ . The difference between  $n_3^{(AF)}$  with  $H_{\text{appl}} > 0$  and  $n_3^{(F)}$  with  $H_{\text{appl}} < 0$  arises from the dependence of the switching time of  $\mathbf{m}_1$  on the direction of  $H_{\text{appl}}$ , and becomes negligible as  $I$  approaches  $I_{c1}$  because the total switching time is mainly determined by that of  $\mathbf{m}_2$  within the limit of  $I/I_{c1} \rightarrow 1$ , as mentioned in Sec. III. For the strong coupling limit, the switching times of the F-coupled and the AF-coupled synthetic free layers are the same because the coupling energy is constant during the switching in this limit, and the coupling field  $H_J$  plays no role on the switching.

Second, we discuss the dependence of the thermal stability  $\Delta$  on the current  $I$ . As shown in Eqs. (12) and (21), our calculations show that  $\Delta \propto \Delta_0(1 - I/I_c)^2$ . It should be noted that our formula is applicable to the single free layer by omitting the coupling of the  $F_1$  and the  $F_2$  layers, and thus, even for the single free layer we find that  $\Delta \propto \Delta_0(1 - I/I_c)^2$ . Recently, a similar result was obtained by Suzuki *et al.*<sup>20</sup> and Butler *et al.*<sup>23</sup> for the perpendicularly magnetized single free layer. However, the formula of the switching rate with  $\Delta \propto \Delta_0(1 - I/I_c)$  first obtained by Koch *et al.*<sup>11</sup> has been widely used to fit the experiments<sup>8-10</sup>.

The important point is that the difference of the exponent of  $(1 - I/I_c)$  leads to a significant underestimation of  $\Delta_0$ . Let us consider the fit of the experimental results of the switching rate with the formula  $P = 1 - \exp\{-f_0 t \exp[-\Delta_0(1 - I/I_c)^n]\}$ , where for simplicity we assume that the attempt frequency  $f_{ij}$  is constant  $f_0$ . When  $I/I_c = 0.5$ , the thermal stability  $\Delta_0$  estimated by our formula ( $n = 2$ ) is two times larger than that estimated by the conventional formula ( $n = 1$ ).

The difference between the exponent of  $(1 - I/I_c)$  in our calculation and that in the theory of Koch *et al.*<sup>11</sup>

arises from the steady-state solution of the Fokker-Planck equation of the free layer magnetization:

$$\frac{\partial W}{\partial t} = \frac{\alpha\gamma}{MV} \frac{1}{\sin\theta} \frac{\partial}{\partial\theta} \left[ \sin\theta \left\{ \left( \frac{\partial F}{\partial\theta} + \frac{a_J MV}{\alpha} \sin\theta \right) W + k_B T \frac{\partial W}{\partial\theta} \right\} \right]. \quad (28)$$

Koch *et al.* argued that the steady-state solution of Eq. (28) is  $W_{\text{Koch}} \propto \exp\{-F[1 + a_J/(\alpha H)]/(k_B T)\}$ , where  $H = |\mathbf{H}|$  is the absolute value of the magnetic field acting on the free layer magnetization. However, when  $H$  depends on  $\mathbf{m}$ ,  $W_{\text{Koch}}$  is *not* a steady state solution of Eq. (28). In general,  $H$  depends on  $\mathbf{m}$  because of the presence of the uni-axial anisotropy field  $\mathbf{H}_{\text{an}} = H_{\text{an}} m_z \mathbf{e}_z$ , which guarantees two local minima of the free energy  $F$ . Thus, in the calculation of the switching rate, we should use  $W_0 \propto \exp\{-[1 - (a_J MV \cos\theta)/(\alpha F)]/(k_B T)\}$ , which is the steady state solution of Eq. (28) as shown in Sec. II, instead of  $W_{\text{Koch}}$ . The difference between  $W_0$  and  $W_{\text{Koch}}$  leads to that of the exponent of  $(1 - I/I_c)$  in  $\Delta$ .

## VI. CONCLUSIONS

In conclusion, we studied the magnetization switching of the synthetic free layer theoretically by solving the Fokker-Planck equation. We obtained the analytical expression of the switching rate for the weak and the strong coupling limits, given by Eqs. (19) and (27). We found that the switching time within the weak coupling limit becomes saturated as the current  $I$  approaches the critical current  $I_{c1}$ . We compared the switching time of the ferromagnetically and the anti-ferromagnetically coupled synthetic free layers with a finite applied field, and find that fast switching is achieved by choosing the appropriate direction of the applied field. We also found that the dependence of the thermal stability on the current is  $\Delta \propto \Delta_0(1 - I/I_c)^2$ , not  $\Delta \propto \Delta_0(1 - I/I_c)$  as argued by previous authors<sup>11</sup>, which leads to a significant underestimation of  $\Delta_0$ .

## ACKNOWLEDGMENT

The authors would like to acknowledge H. Kubota, S. Yuasa, K. Seki, M. Marthaler and D. S. Golubev for valuable discussions. This work was supported by JSPS and NEDO.

## APPENDIX A: DETAILS OF THE CALCULATION IN SEC. III

In this appendix, we show the details of the derivation of Eq. (19) [see also Sec. 4 C in Ref.<sup>14</sup>]. First, let us consider the switching from region 1 to region 2.

The number of the particle in region 1 is obtained by integrating  $2W_1 \exp[-\{\mathcal{F}(\theta_1, 0) - \mathcal{F}(0, 0)\}/(k_B T)]$  over  $0 \leq \theta_{m1} \leq \theta_{m1}$ ; that is,

$$n_1 = 2W_1 e^{\mathcal{F}(0,0)/(k_B T)} \int_0^{\theta_{m1}} d\theta_1 \sin\theta_1 \exp\left[-\frac{\mathcal{F}(\theta_1, 0)}{k_B T}\right]. \quad (29)$$

It should be noted that the exponential term in the integral rapidly decreases by changing  $\theta_1$  from 0 to  $\theta_{m1}$ . Then, we replace  $\mathcal{F}(\theta_1, 0)$  by its Taylor series about  $\theta_1 = 0$ , keep the terms up to the second order of  $\theta_1$ , and replace the upper limit of the integral by  $\infty$ . The first term of Taylor series,  $\partial\mathcal{F}(0, 0)/\partial\theta_1$ , is zero because  $\theta_1 = 0$  corresponds to the local minimum of  $\mathcal{F}$ .  $\sin\theta_1$  is approximated to  $\theta_1$ . Then, we arrive Eq. (7). The number of the particle in region 2,  $n_2$ , is obtained in a similar way; that is,  $n_2 = 2W_2 e^{\mathcal{F}(\pi,0)/(k_B T)} I_2$ , where  $I_2$  is given by

$$I_2 = e^{-\mathcal{F}(\pi,0)/(k_B T)} \frac{k_B T}{\partial^2 \mathcal{F}(\pi, 0)/\partial\theta_1^2}. \quad (30)$$

The particle flow from region 1 to region 2,  $I_{1 \rightarrow 2}$ , satisfies [see Eq. (8)]

$$\frac{\partial W}{\partial\theta_1} + \frac{1}{k_B T} \frac{\partial\mathcal{F}}{\partial\theta_1} W = - \left( \frac{M_1 V_1}{\alpha_1 \gamma_1 k_B T} \right) \frac{I_{1 \rightarrow 2}}{2 \sin\theta_1}. \quad (31)$$

According to Brown<sup>14</sup>, we assume that  $I_{1 \rightarrow 2}$  is independent of  $\theta_1$ . By multiplying  $e^{\mathcal{F}(\theta_1,0)/(k_B T)}$  to Eq. (31) and integrating it over  $[0, \pi]$ , the left hand side of Eq. (31) is reduced to

$$\begin{aligned} & \int_0^\pi d\theta_1 \frac{\partial}{\partial\theta_1} W e^{\mathcal{F}(\theta_1,0)/(k_B T)} \\ &= W(\pi, 0) e^{\mathcal{F}(\pi,0)/(k_B T)} - W(0, 0) e^{\mathcal{F}(0,0)/(k_B T)} \\ &= \frac{1}{2} \left( \frac{n_2}{I_2} - \frac{n_1}{I_1} \right), \end{aligned} \quad (32)$$

where we use the definitions of  $I_1$  and  $I_2$ , i.e.,  $n_1 = 2W_1 e^{\mathcal{F}(0,0)/(k_B T)} I_1$  and  $n_2 = 2W_2 e^{\mathcal{F}(\pi,0)/(k_B T)} I_2$ . On the other hand, by using Taylor series of  $\mathcal{F}(\theta_1, 0)$  about  $\theta_1 = \theta_{m1}$ , the right hand side of Eq. (31) is approximated to  $-[M_1 V_1 / (2\alpha_1 \gamma_1 k_B T)] I_{1 \rightarrow 2} I_{m1}$ , where  $I_{m1}$  is given by Eq. (9). Thus, we obtain

$$\frac{1}{2} \left( \frac{n_2}{I_2} - \frac{n_1}{I_1} \right) = - \frac{M_1 V_1}{2\alpha_1 \gamma_1 k_B T} I_{1 \rightarrow 2} I_{m1}. \quad (33)$$

Similarly, the number of the particles in regions 2 and 3,  $n_2$  and  $n_3$ , and the particle flow from the region 2 to region 3,  $I_{2 \rightarrow 3}$ , satisfy

$$\frac{1}{2} \left( \frac{n_3}{I'_3} - \frac{n_2}{I'_2} \right) = - \frac{M_2 V_2}{2\alpha_2 \gamma_2 k_B T} I_{2 \rightarrow 3} I_{m2}, \quad (34)$$

where  $I'_2$ ,  $I'_3$ , and  $I_{m2}$  are, respectively, given by

$$I'_2 = e^{-\mathcal{F}(\pi,0)/(k_B T)} \frac{k_B T}{\partial^2 \mathcal{F}(\pi, 0)/\partial\theta_2^2}, \quad (35)$$



$$I'_3 = e^{-\mathcal{F}(\pi, \pi)/(k_B T)} \frac{k_B T}{\partial^2 \mathcal{F}(\pi, \pi)/\partial \theta_2^2}, \quad (36)$$

$$I_{m2} = \sqrt{-\frac{2\pi k_B T}{\partial^2 \mathcal{F}(\pi, \theta_{m2})/\partial \theta_2^2} \frac{e^{\mathcal{F}(\pi, \theta_{m2})/(k_B T)}}{\sin \theta_{m2}}}, \quad (37)$$

where  $\theta_{m2} = \cos^{-1}[-(H_{\text{appl}} - H_{J2})/H_{\text{an2}}]$ .

By using Eqs. (33), (34) and the continuity equations of the particle flows,  $\dot{n}_1 = -I_{1 \rightarrow 2}$ ,  $\dot{n}_2 = I_{1 \rightarrow 2} - I_{2 \rightarrow 3}$ , and  $\dot{n}_3 = I_{2 \rightarrow 3}$ , we obtain Eq. (10). The switching probabilities per unit time,  $\nu_{ij}$ , are given by

$$\nu_{12} = \left( \frac{\alpha_1 \gamma_1 k_B T}{M_1 V_1} \right) \frac{1}{I_1 I_{m1}}, \quad (38)$$

$$\nu_{21} = \left( \frac{\alpha_1 \gamma_1 k_B T}{M_1 V_1} \right) \frac{1}{I_2 I_{m1}}, \quad (39)$$

$$\nu_{23} = \left( \frac{\alpha_2 \gamma_2 k_B T}{M_2 V_2} \right) \frac{1}{I'_2 I_{m2}}, \quad (40)$$

$$\nu_{32} = \left( \frac{\alpha_2 \gamma_2 k_B T}{M_2 V_2} \right) \frac{1}{I_3 I_{m2}}. \quad (41)$$

The explicit forms of  $\nu_{ij}$  are obtained by using  $\mathcal{F}(\theta_1, \theta_2)$  and its derivative, and given by Eqs. (11)-(14).

By applying the negative current and magnetic field, which induce the magnetization reversal from  $\mathbf{m}_1, \mathbf{m}_2 = +\mathbf{e}_z$  to  $\mathbf{m}_1, \mathbf{m}_2 = -\mathbf{e}_z$ ,  $\nu_{12}$  and  $\nu_{23}$  become much larger than  $\nu_{21}$  and  $\nu_{32}$ , respectively. Then, Eq. (10) can be approximated to  $\dot{n}_1 = -\nu_{12} n_1$ ,  $\dot{n}_2 = \nu_{12} n_1 - \nu_{23} n_2$  and  $\dot{n}_3 = \nu_{23} n_2$ . Then, the solutions of  $n_1$ ,  $n_2$ , and  $n_3$  with the initial conditions,  $n_1(0) = 1$ ,  $n_2(0) = 0$ , and  $n_3(0) = 0$ , are given by Eqs. (17)-(19).

- 
- <sup>1</sup> J. C. Slonczewski, J. Magn. Magn. Mater. **159**, L1 (1996).  
<sup>2</sup> J. C. Slonczewski, Phys. Rev. B **39**, 6995 (1989).  
<sup>3</sup> L. Berger, Phys. Rev. B **54**, 9353 (1996).  
<sup>4</sup> J. A. Katine, F. J. Albert, R. A. Buhrman, E. B. Myers, and D. C. Ralph, Phys. Rev. Lett. **84**, 3149 (2000).  
<sup>5</sup> S. I. Kiselev, J. C. Sankey, I. N. Krivorotov, N. C. Emley, R. J. Schoelkopf, R. A. Buhrman, and D. C. Ralph, Nature **425**, 380 (2003).  
<sup>6</sup> Y. Huai, F. Albert, P. Nguyen, M. Pakala, and T. Valet, Appl. Phys. Lett. **84**, 3118 (2004).  
<sup>7</sup> G. D. Fuchs, N. C. Emley, I. N. Krivorotov, P. M. Braganca, E. M. Ryan, S. I. Kiselev, J. C. Sankey, D. C. Ralph, R. A. Buhrman, and J. A. Katine, Appl. Phys. Lett. **85**, 1205 (2004).  
<sup>8</sup> J. Hayakawa, S. Ikeda, K. Miura, M. Yamanouchi, Y. M. Lee, R. Sasaki, M. Ichimura, K. Ito, T. Kawahara, R. Take-mura, T. Meguro, F. Matsukura, H. Takahashi, H. Matsuoka, and H. Ohno, IEEE. Trans. Magn. **44**, 1962 (2008).  
<sup>9</sup> S. Yakata, H. Kubota, T. Sugano, T. Seki, K. Yakushiji, A. Fukushima, S. Yuasa, and K. Ando, Appl. Phys. Lett. **95**, 242504 (2009).  
<sup>10</sup> S. Yakata, H. Kubota, T. Seki, K. Yakushiji, A. Fukushima, S. Yuasa, and K. Ando, IEEE. Trans. Magn. **46**, 2232 (2010).  
<sup>11</sup> R. H. Koch, J. A. Katine, and J. Z. Sun, Phys. Rev. Lett. **92**, 088302 (2004).  
<sup>12</sup> Z. Li and S. Zhang, Phys. Rev. B **69**, 134416 (2004).  
<sup>13</sup> D. M. Apalkov and P. B. Visscher, Phys. Rev. B **72**, 180405 (2005).  
<sup>14</sup> W. F. B. Jr, Phys. Rev. **130**, 1677 (1963).  
<sup>15</sup> The spin transfer torque switching in the synthetic free layer is performed at room temperature using an Ru layer with a thickness of a few nm<sup>8-10</sup>. The spin diffusion length of Ru at 4.2 K is 14 nm<sup>22</sup> and it would be much smaller at room temperature.  
<sup>16</sup> Private communication with Hitoshi Kubota. It was experimentally shown that the critical current of the spin transfer torque switching in a CoFeB/Ru/CoFeB spin-valve is one order of magnitude larger than that in CoFeB/MgO/CoFeB MTJs (unpublished). This result means that the spin transfer torque arising between the free layers of the synthetic structure is negligible compared to that arising from the spin current injected from the fixed layer.  
<sup>17</sup> A. Brataas, Y. V. Nazarov, and G. E. W. Bauer, Eur. Phys. J. B **22**, 99 (2001).  
<sup>18</sup> S. Zhang, P. M. Levy, and A. Fert, Phys. Rev. Lett. **88**, 236601 (2002).  
<sup>19</sup> M. Oogane, T. Wakitani, S. Yakata, R. Yilgin, Y. Ando, A. Sakuma, and T. Miyazaki, Jpn. J. Appl. Phys. **45**, 3889 (2006).  
<sup>20</sup> Y. Suzuki, A. A. Tulapurkar, and C. Chappert, *Nanomagnetism and Spintronics* (Elsevier, 2009), Chapter 3.  
<sup>21</sup> Private communication with Hitoshi Kubota and Shinji Yuasa.  
<sup>22</sup> J. Bass and J. W. P. Pratt, J. Phys.: Condens. Matter **19**, 183201 (2007).  
<sup>23</sup> Private communication with C. Mewes. Their results were recently presented at 55<sup>th</sup> Annual Conference on Magnetism and Magnetic Materials by W. Butler (HC-09).